

SUPPLEMENTAL DATA

General

All reagents and solvents were obtained from commercial sources (Sigma-Aldrich, Acros, Biosolve, ABCR, Invitrogen, and Merck for reagents; Biosolve, Merck and Cambridge Isotope Laboratories for normal and deuterated solvents) and used without further purification unless stated otherwise. Polystyrene microspheres (Polybeads, 0.5 μm) were purchased from Polysciences. [^{111}In]Indium chloride, [^{177}Lu]lutetium chloride and sodium [^{125}I]iodide solutions were purchased from PerkinElmer. Water was distilled and deionized (18 M Ωcm) by means of a milli-Q water filtration system (Millipore). The labeling buffers were treated with Chelex-100 resin (BioRad Laboratories) overnight, filtered through 0.22 μm and stored at 4°C. The Bolton-Hunter reagent (N-succinimidyl-3-[4-hydroxyphenyl]propionate, SHPP), kits for bicinchoninic acid (BCA) assay, gelcode blue protein staining solutions and Zeba desalting spin columns (7 kDa and 40 kDa MW cut-off, 0.5-2 mL) were purchased from Pierce Protein Research (Thermo Fisher Scientific). Amicon Ultra-4 and Ultra-15 centrifugal filter units (30 and 50 kDa MW cut-off) were purchased from Millipore. Mouse serum and mouse serum albumin (MSA) were purchased from Innovative Research.

Materials and Methods

NMR spectra were recorded in CDCl_3 or $[\text{D}_6]\text{DMSO}$, using a Bruker DPX300 spectrometer or a Bruker Avance400 spectrometer. ^{13}C NMR multiplicities (q = quaternary, t = tertiary, s = secondary and p = primary) were distinguished using a DEPT pulse sequence. Infrared spectra were measured on a PerkinElmer 1600 FT-IR. MALDI-TOF mass spectra (positive, linear mode) of the albumin-conjugates were acquired on a Voyager – DETM Pro (PerSeptive Biosystems, PE) using a matrix of α -cyano-4-hydroxy-cinnamic acid (CHCA). Preparative column chromatography was performed on a Combiflash Companion apparatus (Teledyne Isco) using SiliCycle silica columns. Analytical radio-HPLC was carried out on an Agilent 1100 system equipped with a Gabi radioactive detector (Raytest). Radioactivity was counted in a gamma counter (Wizard 1480, PerkinElmer): tissues from single-isotope experiments were measured using 10-80 keV, 10-380 keV, and 150-500 keV energy windows for ^{125}I , ^{177}Lu , and ^{111}In , respectively; tissues from dual-isotope experiments were measured using dual-isotope protocol (10-80 keV and 155-380 keV energy windows for ^{125}I and ^{177}Lu , respectively, with cross-contamination correction).

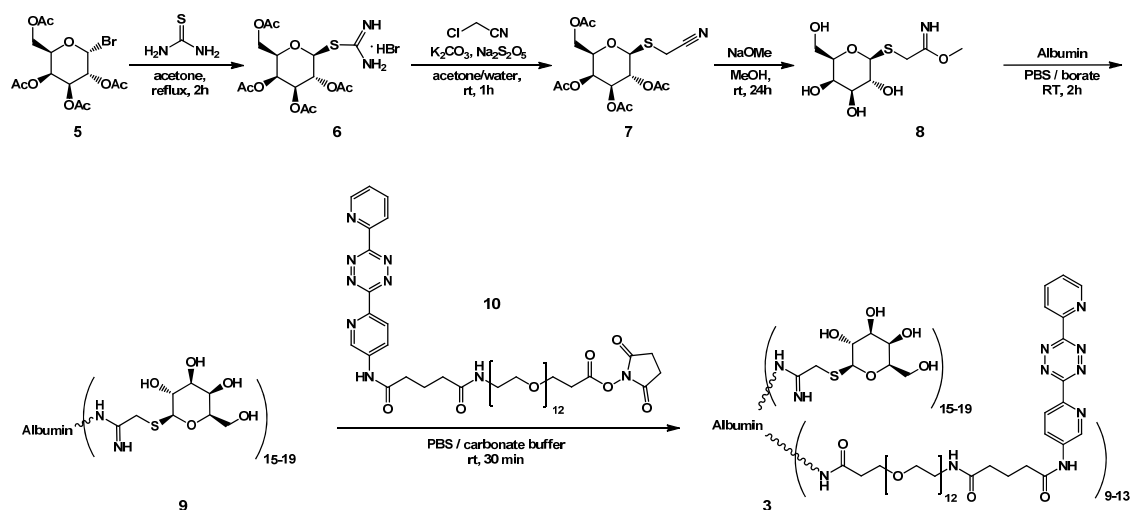
The ^{111}In - and ^{177}Lu -labeling yields were determined by radio-TLC, using ITLC-SG strips (Varian Inc.) eluted with 200 mM EDTA in saline and imaged on a phosphor imager (FLA-7000, Fujifilm). In these conditions, free ^{111}In and ^{177}Lu migrate with $R_f = 0.9$, while $^{111}\text{In}/^{177}\text{Lu}$ -tetrazine and ^{177}Lu -DOTA-CC49 remain at the origin. The radiochemical purity of the ^{111}In - and ^{177}Lu -labeled tetrazine **2** was determined by radio-HPLC on an Agilent 1100 system equipped with a Gabi radioactive detector (Raytest). The samples were loaded on an Agilent Eclipse XDB-C18 column ($4.6 \times 150\text{mm}$, $5\mu\text{m}$), which was eluted at 1 mL/min with a linear gradient of acetonitrile in water containing 0.1% TFA (2 min at 10% acetonitrile followed by an increase to 45% acetonitrile in 11 min). The UV wavelength was preset at 254 nm. The ^{125}I -mAb labeling yields were also determined with radio-TLC, using ITLC-SG strips eluted with a 1:1 methanol/ethylacetate mixture and imaged on a phosphor imager. In these conditions, free [^{125}I]iodide and ^{125}I -SHPP migrate with $R_f = 0.5$ - 0.9 , while ^{125}I -mAbs remain at the origin. The radiochemical purity of ^{125}I -CC49-TCO and ^{177}Lu -DOTA-CC49 was determined by Size Exclusion (SEC) HPLC and SDS-PAGE. SEC-HPLC was carried out on an Agilent 1200 system equipped with a Gabi radioactive detector. The samples were loaded on a Superdex 200 10/300 column (GE Healthcare Life Sciences) and eluted with 10 mM phosphate buffer pH 7.4 at 0.5 mL/min. The UV

wavelength was preset at 260 and 280 nm. SDS-PAGE was performed on a Phastgel system using 7.5% PAGE homogeneous gels (GE Healthcare Life Sciences). The number of tetrazine molecules conjugated to albumin and the concentration of CC49 solutions were determined with a NanoDrop 1000 spectrophotometer (Thermo Fisher Scientific) from the absorbance at 322 nm and 280 nm, respectively. The number of tetrazines per albumin molecule was also determined by MALDI-TOF. The concentration of CC49 solutions was also determined by BCA assay. The average hydrodynamic diameter of the polystyrene beads coated with albumin-tetrazine was determined by dynamic light scattering (ALV-LSE, $\alpha = 90^\circ$). The absence of aggregates in the bead suspension and the number of beads injected in mice were determined with a Beckman Coulter Counter (Multisizer 3) using a 50 μm aperture tube. An aliquot of the solution was mixed with 50 mL Isoton II (Beckman Coulter) from which 100 μL was analyzed in the diameter range of 1.1 μm to 30 μm .

The human colon cancer cell line LS174T was obtained from the ATCC and maintained in Eagle's minimal essential medium (Sigma) supplemented with 10% heat inactivated fetal calf serum (Gibco), penicillin (100 U/mL), streptomycin (100 $\mu\text{g}/\text{mL}$) and 2 mM Glutamax. At the time of mAb injection the size of the tumors of the mice receiving directly labeled mAb was

approximately 150-200 mm³ while those of the pretargeted animals was approximately 70-100 mm³ (to compensate for the additional time until radioactivity injection).

Clearing Agent Development



Supplemental Figure 1: Synthesis of galactose-albumin-tetrazine (3)

2-S-(2,3,4,6-Tetra-O-Acetyl- β -D-Galactopyranosyl)-2-Thiouronium

Bromide (6). 2,3,4,6-Tetra-O-acetyl- α -D-galactopyranosyl bromide (**5**; 15.00 g, 36.48 mmol) and thiourea (3.05 g, 40.07 mmol) were dissolved in acetone (75 mL). The solution was heated to reflux for 2 h, and subsequently filtered and cooled to 20°C. Addition of pentane (75 mL) resulted in the precipitation of the

product as a white, crystalline solid (16.11 g, 91%). ¹H-NMR (400 MHz, [D₆]DMSO): δ = 9.35 (br, 2H, NH₂), 9.11 (br, 2H, NH₂), 5.71 (d, *J*_{1,2} = 10 Hz, 1H, H₁), 5.39 (d, *J* = 3.2 Hz, 1H, H₄), 5.22 (dd, *J*_{2,3} = 9.9 Hz, *J*_{3,4} = 3.2 Hz, 1H, H₃), 5.11 (t, *J*_{2,3} = 10 Hz, 1H, H₂), 4.45 (t, *J* = 6.4 Hz, 1H, H₅), 4.09 (m, 2H, H₆, H_{6'}), 2.14 (s, 3H, CH₃), 2.08 (s, 3H, CH₃), 2.01 (s, 3H, CH₃), 1.95 (s, 3H, CH₃) ppm.

Cyanomethyl 2,3,4,6-Tetra-O-Acetyl-1-Thio-β-D-Galactopyranoside (7).

Compound **6** (16.11 g, 31.07 mmol), sodium metabisulphite (11.81 g, 62.14 mmol), potassium carbonate (4.72 g, 34.18 mmol), and chloroacetonitrile (8.21 g, 108.7 mmol) were dissolved in acetone/water (50:50 v/v, 200 mL), and stirred for 1 h at room temperature. The reaction mixture was poured in iced water (300 mL) and stirred for an additional 2 h. The white precipitate was collected by filtration and recrystallized from hot methanol (30 mL). The product was filtered off as a white crystalline solid (9.61 g, 77%). M.p. = 97°C (Lit: 95-97°C). ¹H-NMR (400 MHz, CDCl₃): δ = 5.47 (d, *J* = 2.4 Hz, 1H, H₄), 5.24 (t, *J* = 10 Hz, 1H, H₂), 5.11 (dd, *J*_{3,4} = 3.2 Hz, *J*_{2,3} = 10 Hz, 1H, H₃), 4.7 (d, *J*_{1,2} = 10 Hz, 1H, H₁), 4.16 (m, 2H, H₆, H_{6'}), 4.01 (t, *J* = 6.9 Hz, 1H, H₅), 3.64 (d, *J* = 17 Hz, 1H, S-CH'), 3.35 (d, *J* = 17 Hz, 1H, S-CH), 2.17 (s, 3H, CH₃),

2.09 (s, 3H, CH₃), 2.07 (s, 3H, CH₃), 2.00 (s, 3H, CH₃) ppm. FT-IR (ATR): ν = 2249 (CN, w), 1739 (C=O, s).

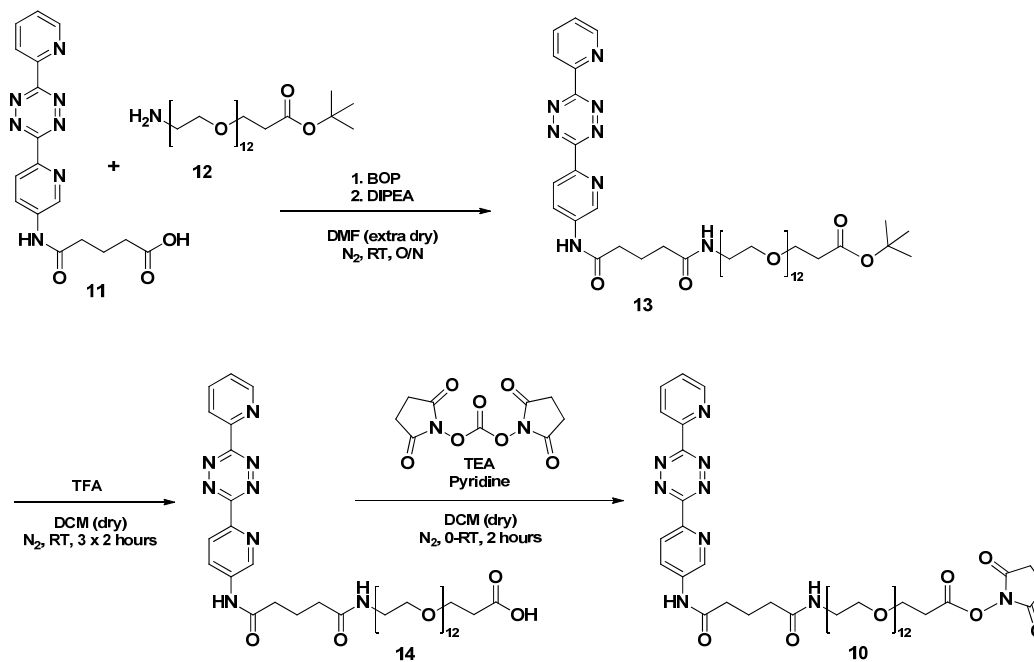
2-Imino-2-Methoxyethyl-1-Thio- β -D-Galactopyranoside (8). Compound **7** (2.02 g, 5.00 mmol) was dissolved in anhydrous methanol (50 mL) and a methanolic solution of sodium methoxide (25 w%, 115 μ L, 0.50 mmol) was added. The reaction mixture was stirred at room temperature for 24 h and subsequently concentrated to a 15 mL volume. The product was allowed to crystallize at room temperature and then at -18°C. Filtration and drying gave white crystals (1.11 g; 83%). M.p. = 129°C. ¹H-NMR (400 MHz, CD₃OD): δ = 4.27 (d, $J_{1,2}$ = 9.6 Hz, 1H, H₁), 3.87 (dd, $J_{3,4}$ = 4.0 Hz, $J_{4,5}$ = 1.5 Hz, 1H, H₄), 3.78 (m, 2H, H₆, H_{6'}), 3.73 (s, 3H, -OCH₃), 3.54 (m, 1H, H₅), 3.52 (dd, $J_{2,3}$ = 10 Hz, $J_{1,2}$ = 9.0 Hz, 1H, H₂), 3.44 (dd, $J_{2,3}$ = 10 Hz, $J_{3,4}$ = 4.2 Hz, 1H, H₃) ppm. FT-IR (ATR): ν = 3287 (N-H, s), 1650 (C=NH, s).

Galactose-Albumin (9). Galactose conjugation to mouse serum albumin (MSA) was performed with a reactive imino-derivative **8** directly coupled to MSA via the terminal amino-groups of its Lys residues. A freshly-prepared 18.2 mg/mL stock solution of **8** in a 9:1 mixture of PBS pH 7.4/0.5 M borate buffer pH 8.5 (200 μ L) was added to a solution of MSA (20 mg, 0.30 μ mol,

Innovative Research) in the same buffer (900 μL), resulting in a 45-fold molar excess of galactose coupling agent (**8**) relative to albumin. The reaction mixture was shaken (500 rpm) at room temperature for 2 h. The low MW components were eliminated using a Zeba desalting spin column (7 kDa MW cut-off, Pierce Protein Research) pre-equilibrated with water. After freeze-drying, galactose-MSA was obtained as a white fluffy solid (15.3 mg, 0.22 μmol , 72%), which was further purified by size exclusion chromatography to remove albumin oligomers (already present in native albumin). The galactose modification grade was subsequently determined by MALDI-TOF analysis. MSA: $[M+H^+] = 65941$ m/z . Galactose-MSA: $[M+H^+] = 69823$ m/z , which corresponds to a mean of 16.4 galactoses/MSA. Variation among different batches is 15-18 galactoses/MSA. The stability of a 10 mg/mL solution of **9** in water at 4°C was assessed by repeated MALDI-TOF analysis every 2 weeks for a total of 5 months. The conjugate proved to be stable.

Synthesis of Galactose-Albumin-Tetrazine (3). The galactose-functionalized albumin **9** was then modified with tetrazine moieties via its Lys residues. A solution of **9** (1 mg) in PBS was mixed with a 10 mg/mL solution of tetrazine-NHS (**10**) in DMF (30 μL , 20 eq. with respect to **9**) and 1 M sodium carbonate

buffer pH 9.6 (7.5 μL) was added. The solution (250 μL total) was incubated at room temperature for 30 min and then transferred into an Amicon Ultra-15 centrifugal filter unit (30 kDa MW cut-off, Millipore) and product **3** was washed extensively with water. After overnight freeze-drying, **3** was obtained as a pink fluffy powder. The tetrazine modification grade was determined by MALDI-TOF analysis. Galactose-MSA-tetrazine: $[M+H^+] = 79010$ m/z , which corresponds to a mean of 9.7 tetrazines/ galactose(16.4)-MSA. UV-Vis measurements confirmed the presence of 9 tetrazines per molecule (measured value: 8.9 tetrazines/ galactose(16.4)-MSA). Variation among different batches is 9-13 tetrazines per MSA-galactose.



Supplemental Figure 2: Synthesis of 2,5-dioxopyrrolidin-1-yl 41,45-dioxo-45-((6-(6-(pyridin-2-yl)-1,2,4,5-tetrazin-3-yl)pyridin-3-yl)amino)-4,7,10,13,16,19,22,25,28,31,34,37-dodecaoxa-40-azapentatetracontan-1-oate (**10**, tetrazine-NHS)

The synthesis of tetrazine-NHS (**10**) starts from 5-oxo-5-(6-(6-(pyridin-2-yl)-1,2,4,5-tetrazin-3-yl)pyridin-3-ylamino)pentanoic acid (**11**), which was made according to a published method (*1*).

Tert-Butyl 41,45-Dioxo-45-((6-(6-(Pyridin-2-yl)-1,2,4,5-Tetrazin-3-yl)Pyridin-3-yl)Amino)-4,7,10,13,16,19,22,25,28,31,34,37-Dodecaoxa-40-Azapentatetracontan-1-oate (13). Tert-butyl 1-amino-3,6,9,12,15,18,21,24,27,30,33,36-dodecaoxanonatriacontan-39-oate **12** (123 mg, 0.182 mmol; IRIS Biotech GmbH) was added into a dried reaction vial and co-evaporated twice with toluene. The vial was then put under N₂ and extra dry DMF (2 mL) was added giving a colorless solution. Compound **11** (100 mg, 0.274 mmol) and BOP (267 mg, 0.603 mmol) dissolved in extra dry DMF (1 mL) were added sequentially to the reaction mixture under N₂ atmosphere giving a red suspension. Finally, DIPEA (0.5 mL, 2.74 mmol) was added dropwise to the reaction mixture and the resulting solution was stirred overnight. The reaction mixture was evaporated to dryness, dissolved in dichloromethane (2 mL), and purified by flash column chromatography on silica gel using a gradient of 1-10% methanol in dichloromethane. The relevant fractions were combined and evaporated in vacuo yielding **13** (167 mg, 0.164 mmol, 90%) as a dark pink solid. ¹H NMR (300 MHz, CDCl₃): δ = 10.58 (s, 1H), 9.05 (d, *J* = 2.4 Hz, 1H), 8.93 (ddd, *J*₁ = 0.9 Hz, *J*₂ = 1.7 Hz, *J*₃ = 4.7 Hz, 1H), 8.62 (d, *J* = 8.8 Hz, 1H), 8.59 (d, *J* = 8.6 Hz, 1H), 8.43 (dd, *J*₁ = 2.4 Hz, *J*₂ = 8.8 Hz, 1H), 8.15 (td, *J*₁ = 1.8 Hz, *J*₂ = 7.8 Hz, 1H), 7.93 (t, *J* = 5.5 Hz, 1H), 7.73 (ddd, *J*₁ = 1.1 Hz, *J*₂ = 4.7 Hz, *J*₃ = 7.8 Hz, 1H), 3.57 (t, *J* = 6.2 Hz, 2H),

3.53-3.47 (broad s, 46H), 3.25-3.16 (m, 2H), 3.41 (t, $J = 6.2$ Hz, 2H), 2.44 (t, $J = 7.3$ Hz, 2H), 2.17 (t, $J = 7.3$ Hz, 2H), 1.85 (q, $J = 7.3$ Hz, 2H), 1.38 (s, 9H) ppm; ^{13}C NMR (75 MHz, CDCl_3): $\delta = 172.1$ (q), 171.7 (q), 170.4 (q), 163.0 (q), 162.8 (q), 150.6 (t), 150.2 (q), 143.8 (q), 141.3 (t), 138.5 (q), 137.8 (t), 126.5 (t), 126.1 (t), 124.8 (t), 124.2 (t), 79.7 (q), 69.8 (s), 69.7 (s), 69.6 (s), 69.5 (s), 69.1 (s), 66.2 (s), 38.5 (s), 35.8 (s), 35.7 (s), 34.4 (s) 27.7 (p), 20.9 (s) ppm.

41,45-Dioxo-45-((6-(6-(Pyridin-2-yl)-1,2,4,5-Tetrazin-3-yl)Pyridin-3-yl)Amino)-4,7,10,13,16,19,22,25,28,31,34,37-Dodecaoxa-40-Azapentatetracontan-1-oic Acid (14). TFA (2 mL) was added to a stirred solution of **13** (160 mg, 0.157 mmol) in anhydrous dichloromethane (2 mL) under N_2 atmosphere. The reaction mixture was stirred for 2 h at room temperature and evaporated to dryness. The residue was redissolved in dry dichloromethane (2 mL) and again treated with TFA (2 mL) for 2 h. This process was repeated once more. Finally, the reaction mixture was evaporated to dryness and co-evaporated twice with dichloromethane yielding the deprotected product **14** in quantitative yield. ^1H NMR (300 MHz, CDCl_3): $\delta = 10.57$ (s, 1H), 9.05 (broad s, 1H), 8.94 (broad s, 1H), 8.63 (d, $J = 8.4$ Hz, 1H), 8.60 (d, $J = 7.2$ Hz, 1H), 8.43 (dd, $J_1 = 2.4$ Hz, $J_2 = 8.8$ Hz, 1H), 8.16 (td, $J_1 = 1.7$ Hz, $J_2 = 7.8$ Hz, 1H), 7.93 (t, $J = 5.5$ Hz, 1H), 7.74 (dd, $J_1 = 4.7$ Hz, $J_3 = 6.8$

Hz, 1H), 3.58 (t, $J = 6.4$ Hz, 2H), 3.53-3.46 (broad s, 46H), 3.41 (t, $J = 6.0$ Hz, 2H), 3.25-3.17 (m, 2H), 2.44 (t, $J = 7.3$ Hz, 2H), 2.17 (t, $J = 7.3$ Hz, 2H), 1.85 (q, $J = 7.3$ Hz, 2H) ppm.

2,5-Dioxopyrrolidin-1-yl 41,45-Dioxo-45-((6-(6-(Pyridin-2-yl)-1,2,4,5-Tetrazin-3-yl)Pyridin-3-yl)Amino)-4,7,10,13,16,19,22,25,28,31,34,37-

Dodecaoxa-40-Azapentatetracontan-1-oate (10). Di-(N-succinimidyl)

carbonate (47.8 mg, 0.187 mmol), pyridine (15 μ L), and TEA (0.25 mL) were added sequentially to a stirred solution of **14** (150 mg, 0.155 mmol) in anhydrous dichloromethane (3 mL) under N₂ atmosphere at 0°C. The mixture was stirred for 2 h while warming up to room temperature, then evaporated to dryness, redissolved in dichloromethane (20 mL), and washed with H₂O (3 \times 10 mL). The organic layer was dried over MgSO₄, filtered and evaporated in vacuo yielding **10** (94 mg, 0.089 mmol, 57%) as a dark pink solid. ¹H NMR (300 MHz, CDCl₃): $\delta = 9.67$ (s, 1H), 9.01-8.97 (m, 2H), 8.77-8.71 (m, 2H), 8.64 (dd, $J_1 = 2.4$ Hz, $J_2 = 8.8$ Hz, 1H), 8.02 (td, $J_1 = 1.7$ Hz, $J_2 = 7.7$ Hz, 1H), 7.58 (ddd, $J_1 = 1.1$ Hz, $J_2 = 4.7$ Hz, $J_3 = 7.5$ Hz, 1H), 6.60 (t, $J = 5.4$ Hz, 1H), 3.84 (t, $J = 6.4$ Hz, 2H), 3.70-3.55 (broad s, 46H), 3.52-3.43 (m, 2H), 2.90 (t, $J = 6.5$ Hz, 2H), 2.85 (s, 4H), 2.58 (t, $J = 6.8$ Hz, 2H), 2.37 (t, $J = 6.8$ Hz, 2H), 2.09 (q, $J = 6.8$ Hz, 2H) ppm; ¹³C NMR (75 MHz, CDCl₃): $\delta = 172.9$ (q), 172.5 (q), 168.9

(q), 166.7 (q), 163.6 (q), 163.4 (q), 151.0 (t), 150.3 (q), 144.0 (q), 142.0 (t), 138.6 (q), 137.4 (t), 126.5 (t), 126.4 (t), 125.1 (t), 124.3 (t), 70.7 (s), 70.5 (s), 70.2 (s), 69.6 (s), 65.7 (s) 39.3 (s), 35.9 (s), 35.0 (s), 32.1 (s) 25.6 (s), 21.3 (s) ppm.

Preparation of Polystyrene Beads Coated with Tetrazine-Conjugated Bovine Serum Albumin (4). A solution of BSA (1.5 mg) in PBS was mixed with a 10 mg/mL solution of tetrazine-NHS (**10**) in DMF (63 μ L, 26 eq. with respect to BSA) and 1 M sodium carbonate buffer pH 9.6 (7.5 μ L) was added. The solution (250 μ L total) was incubated at room temperature for 30 min and then the low MW components were removed from the solution by using a Zeba desalting spin column (7 kDa MW cut-off) pre-washed with PBS. UV measurements confirmed the presence of 8-10 tetrazine moieties per BSA molecule. Then the eluate containing BSA-tetrazine in PBS was added to a 750 μ L suspension of polystyrene beads (Polybeads, 0.5 μ m; Polysciences) in H₂O and the resulting suspension was incubated at room temperature for 1 h on an end-over-end rotating mixer (10 rpm). After incubation, the suspension of beads coated with BSA-tetrazine (**4**) was centrifuged at 12,000 rpm for 4 min. The supernatant was carefully removed and the pellet was resuspended in 1 mL 0.3% BSA in PBS (w/v) by using a tip sonicator at low power (Sonics

VibraCell, 4×5 sec pulses, 40% of power). The centrifuging-resuspension cycle was repeated 3 times to remove unbound tetrazine-BSA, after which the bead pellet was resuspended in 750 μ L 0.3% BSA in PBS. After coating, the diameter of the beads (506 nm, number weighed) was determined by DLS. Before use, the bead suspension was analyzed by DLS and Coulter Counter (99% of particles were smaller than 2.7 μ m).

Clearing agent reactivity in vitro

Clearing agent **3** (4 molar eq. with respect to mAb) was reacted with radiolabeled CC49-TCO in 50% mouse serum. Galactose-MSA (**9**) was used as control. After 10 min incubation at 37°C, SDS-PAGE analysis of the two reaction mixtures showed a shift of >95% of the mAb-related radioactivity to the front of the gel due to the formation of **3**/CC49-TCO aggregates, thus confirming reaction in vitro. The reactivity of **4** towards CC49-TCO was also evaluated in mouse serum. Ca. 4×10^7 beads were incubated with 20 μ g 125 I-CC49-TCO in 80% mouse serum (1 mL) for 20 min at room temperature on an end-over-end rotating mixer (10 rpm). After centrifugation and gamma-counting, 98% of the initial activity was found in the bead pellet confirming reaction with CC49-TCO in serum.

DOTA-CC49 Conjugation

2 mg CC49 was modified with 4 eq. of p-SCN-Bz-DOTA (Macrocyclics, 10 mg/mL in DMSO) in a total volume of 100 μ L 0.1 M NaHCO₃/Na₂HPO₄ buffer pH 8.5. The reaction was carried out under agitation for 3 h at 37°C. Subsequently, the DOTA-CC49 was extensively washed with 0.25 M ammonium acetate buffer pH 7.0 using an Amicon Ultra-4 centrifugal device (50 kDa MW cut-off) and the mAb concentration in the final solution was measured by UV-Vis (Nanodrop). The number of DOTA groups per mAb molecule was calculated by reacting a known amount of DOTA-CC49 with a known excess of LuCl₃ (spiked with radioactive ¹⁷⁷Lu) for 2 h at 37°C and by measuring the % bound Lu through radio-ITLC ($n_{\text{DOTA}} = n_{\text{Lu}} \times \text{reaction yield} / 100$). CC49 reaction with DOTA-NCS afforded an average of 3 DOTAs per mAb.

DOTA-CC49 Radiolabeling

Lutetium-177 labeling of DOTA-CC49 (100 μ g) was carried out in 1 M ammonium acetate pH 5.0 (50 μ L). The labeling mixture was incubated for 1 h at 37°C, then combined with a 10 mM DTPA solution (5 μ L) and incubated for 10 min more. The radiolabeling yield was determined by radio-ITLC and subsequently the crude ¹⁷⁷Lu-DOTA-CC49 was purified twice through Zeba

desalting spin columns (40 kDa MW cut-off). The radiochemical purity of ^{177}Lu -DOTA-CC49 was >98%, as assessed by radio-ITLC, SEC-HPLC and SDS-PAGE. The specific activity was adjusted to ca. 5 kBq/ μg mAb by adding non-radioactive DOTA-CC49 for animal experiments.

Considerations regarding dosing and timing of pretargeting components

We used 100 μg CC49 construct per mouse as this amount was used in our previous study (*1*) and in many other preclinical pretargeting studies. We reduced the amount of injected tetrazine **2** from 17 nmol used in (*1*) to 6.7 nmol/mouse (i.e. 1.2 eq. to TCO) to increase the radioactivity %ID/g in tumor. The clearing agent dose optimization is discussed below. For the first injection of clearing agent we selected 30 h as this should allow for sufficient time for CC49-TCO accumulation on tumor, based on our results in (*1*). For the second injection of clearing agent we chose 48 h to allow for enough time for Ashwell receptor recycling and for practical reasons.

Clearing Agent Dose Optimization

Tumor-bearing mice ($n = 3-4$) were injected with ^{125}I -CC49-TCO (100 $\mu\text{g}/100 \mu\text{L}$ per mouse; ca. 0.4 MBq; $t = 0$) followed by varying amounts of clearing agent **3** (20-200 $\mu\text{g}/\text{mouse}$ in 100 μL ; $t = 24$ h). Two hours after

clearing agent administration the mice were injected with ^{111}In -DOTA-tetrazine **2** (8.52 μg in 75 μL , 3.4 eq. with respect to TCO, ca 0.5 MBq) and 3 h later (29 h post-mAb injection) the animals were sacrificed. Tissues and organs of interest were harvested and the radioactivity was measured with a dual-isotope protocol.

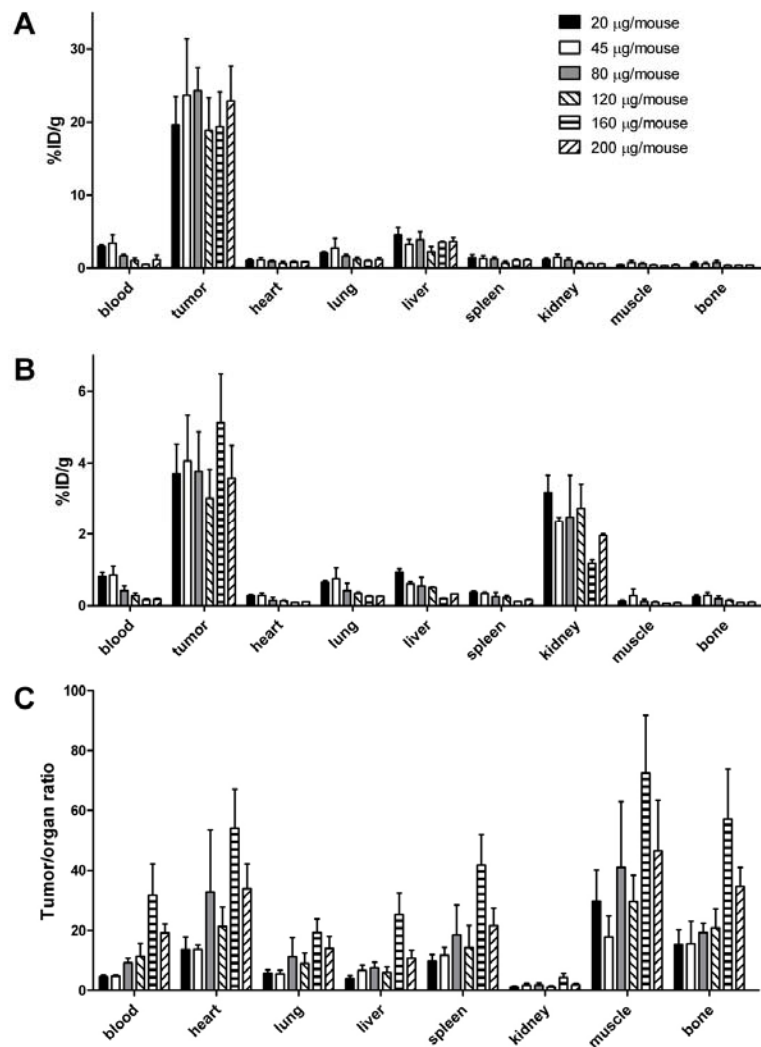
We observed a progressive decrease in circulating mAb with increasing amounts of administered **3** (from 2.92 ± 0.26 %ID/g ^{125}I -CC49-TCO with 20 μg **3** per mouse to 0.53 ± 0.04 %ID/g with a 160 μg dose, Supplemental Fig. 3A). As expected, decreasing retention of ^{111}In -tetrazine in blood was also observed as a consequence of mAb-TCO removal (from 0.81 ± 0.12 to 0.17 ± 0.02 %ID/g, Supplemental Fig. 3B). At the same time, ramping up the **3** dose did not affect the uptake of ^{125}I -mAb in tumor and it did not compromise the reaction between the tumor-bound TCO and the ^{111}In -labeled tetrazine. This is most likely due to the high MW of clearing agent **3**, which hampers extravasation into tumor tissues in the short time between injection and liver capture. Therefore, an increase in T/NT ratios for ^{111}In -tetrazine was observed in all considered organs and tissues with 20-160 μg **3** (Supplemental Fig. 3C).

These findings are different from what was observed by Axworthy et al. in a similar experiment for the biotin system (2). In mice pre-treated with a mAb-streptavidin conjugate, a nadir in blood retention of radiolabeled biocytin

was observed with any tested dose of galactose-HSA-biotin(9) greater or equal to 40 μg per mouse. This was probably due to streptavidin blocking by the excess biotin that was released upon catabolism of the clearing agent. In fact, the mAb-streptavidin that had not been effectively cleared by low doses of clearing agent was still in circulation but had lost its ability to bind biocytin. Also, due to biotin release a concomitant decrease in radioactivity uptake in tumor was observed with high doses of clearing agent. On the contrary, when a galactose-HSA carrying a single biotin moiety was used as clearing agent, Axworthy et al. observed both high biocytin tumor binding and a progressive decrease in biocytin blood uptake over a 90-180 μg dose range (2). In our case, lack of tumor blocking and progressive decrease in tetrazine blood retention support the hypothesis that the excess of tetrazine on **3** is not re-cycled after catabolism or that it is otherwise de-activated in the lysosomal compartment of hepatocytes after interaction with the Ashwell receptors.

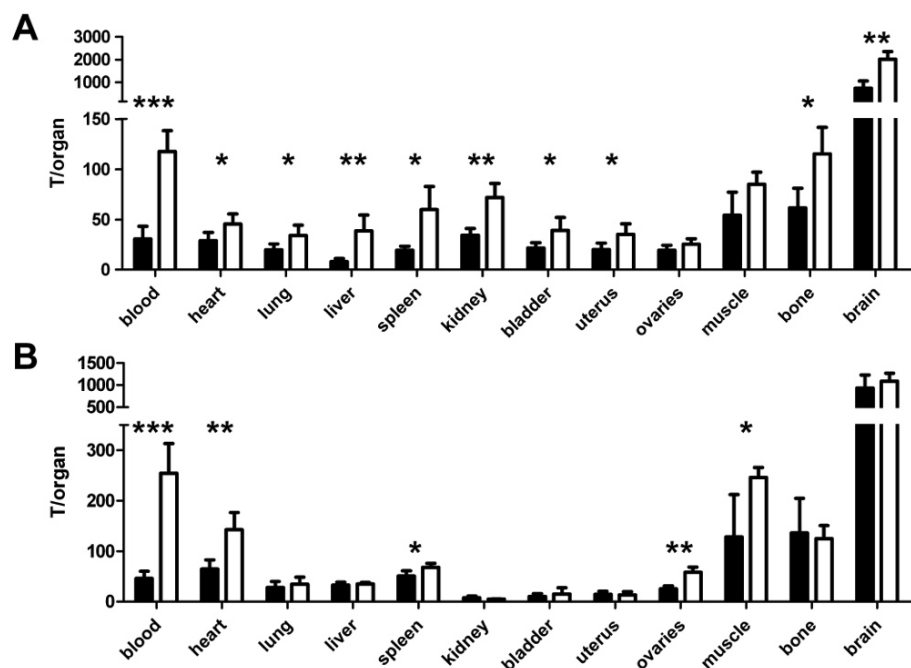
The positive trend observed in the **3** dose range experiment ended at doses exceeding 160 μg per mouse. With 200 μg **3**, the mAb-related radioactivity in blood increased slightly (1.14 ± 0.65 %ID/g vs. 0.53 ± 0.04 %ID/g with 160 μg **3**). However, this did not translate into a higher retention of ^{111}In -tetrazine (0.18 ± 0.02 %ID/g vs. 0.17 ± 0.02 %ID/g with 160 μg **3**). Possibly, the ^{125}I left in blood was due to the **3**/ ^{125}I -CC49-TCO reaction

product, which was not efficiently captured by the liver and was not reactive towards ^{111}In -DOTA-tetrazine. Although galactose-containing constructs are known to bind avidly to Ashwell receptors on hepatocytes and to internalize rapidly into endocytic vesicles, the subsequent dissociation from the receptor is rather slow ($k_{off} < 0.9 \times 10^{-5} \text{ sec}^{-1}$) (3). In view of this potential Ashwell receptor saturation effect, doses of 160 μg **3** per mouse were considered optimal and were used in the following experiments.



Supplemental Figure 3: Clearing agent dose optimization in LS174T tumor-bearing mice injected with ^{125}I -CC49-TCO ($t = 0$) followed by 20-200 μg **3** ($t = 24$ h) and 25 eq. (with respect to mAb) ^{111}In -**2** ($t = 26$ h). Biodistribution of (A) CC49-TCO and (B) tetrazine and (C) tumor-to-organ ratios for tetrazine 3 h post-tetrazine injection. The bars represent the mean \pm SD ($n = 3$ -4).

In mice administered 2 doses of clearing agent **3** between ^{125}I -CC49-TCO and ^{177}Lu -tetrazine **2** we observed a significant increase in tumor-to-organ ratios for both ^{125}I (Supplemental Fig. 4A) and ^{177}Lu (Supplemental Fig. 4B). With respect to our previous experiments without clearing agent (*I*), calculation of the absolute amounts of TCO and tetrazine present in tissues from the %ID/g values of ^{125}I and ^{177}Lu reveal an expected reduction of on-tumor reaction yield (based on TCO) from 52% to 46% (corrected for TCO degradation in vivo; for comparison, in (*I*) the reaction yield corrected for TCO degradation in vivo was 69%) due to the reduced amount of probe used to increase the probe %ID/g (1.2 molar eq. with respect to TCO vs. 6.7 nmol).

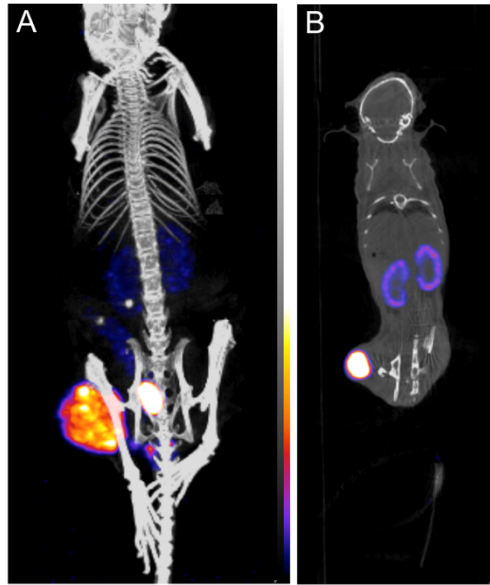


Supplemental Figure 4: Tumor-to-organ ratios from a dual-isotope biodistribution experiment with (A) ^{125}I -CC49-TCO and (B) ^{177}Lu -tetrazine **2** in LS174T tumor-bearing mice treated with one (30 h post-mAb injection, solid bars) or two doses (30 h and 48 h post-mAb injection, empty bars) of galactose-albumin-tetrazine (**3**). The mice were injected with ^{177}Lu -**2** 2 h after the last clearing agent and were euthanized 3 h later. The bars represent the mean tumor-to-organ ratio \pm SD (n = 4; * P < 0.05; ** P < 0.005; *** P < 0.001).

SPECT/CT Imaging

SPECT/CT imaging was carried out on a dedicated small animal SPECT/CT system (NanoSPECT/CT, Bioscan) equipped with 4 detector heads and converging 9-pinhole collimators (pinhole diameter: 1.4 mm). First a CT scan (180 projections; 1000 msec per projection; 45 kV peak tube voltage; 177 mA tube current; 35 mm field of view) and then a SPECT scan (24 projections; 120 sec per projection; photopeaks for ^{111}In set to 171 keV (15% FW) and 245 keV (20% FW)) were performed. Three hours post-tetrazine injection the mouse was euthanized by anesthesia overdose and a high resolution SPECT/CT scan was performed (360 projections and 2000 msec per projection for CT; 36 projections and 300 sec per projection for SPECT). The SPECT images were reconstructed using HiSPECTNG (SciVis GMBH) to an isotropic voxel size of 300 μm . The CT images were reconstructed using InVivoScope (Bioscan) to an isotropic voxel size of 200 μm .

High-resolution post-mortem SPECT imaging showed a heterogeneous signal distribution in the kidney, with most of the activity accumulating in the renal cortex (Supplemental Fig. 5B), possibly due to glomerular filtration and partial retention of the tetrazine in the proximal tubules.



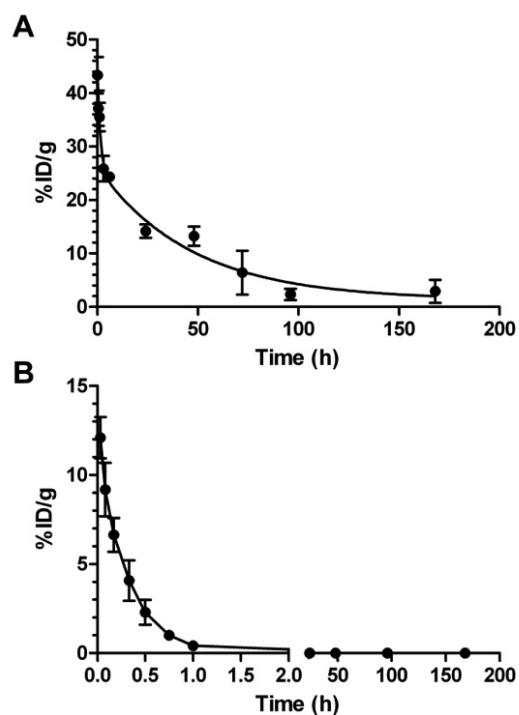
Supplemental Figure 5: SPECT/CT images of a mouse treated with CC49-TCO pretargeted ^{111}In -2. (A) Maximum Intensity Projection of the live mouse 2 h post-tetrazine injection; (B) high resolution post-mortem coronal slice at a higher signal intensity scale to highlight the radioactivity distribution in the kidneys.

Biodistribution and Dosimetry

The tracer %ID for blood, muscle and bone were estimated assuming weights of respectively 6, 42 and 11% of the body weight. The activity measured in the small and large intestines were assigned to the organ content.

Activity to the large intestine was assigned in equal part to the upper and lower large intestines. Activity to the bone was assigned in equal part to the trabecular and spongy bone components. Excretion profiles (combined feces and urine) were generated for ^{177}Lu -DOTA-CC49 and CC49-TCO pretargeted ^{177}Lu -**2** for the first 4 days of the experiment. Mice injected with ^{177}Lu -DOTA-CC49 (n = 4) were housed in filtered cages and at various time points the bedding was counted in a gamma counter along with standards. Another group of mice (n = 4) was injected with ^{177}Lu -**2** at higher specific activity (ca. 12 MBq/8.52 μg **2** per mouse) and whole-body clearance was monitored by measuring the animals in a dose calibrator at various time points. In the mice treated with ^{177}Lu -DOTA-CC49 approximately 50 %ID was not accounted for in the harvested tissues or excreted and was therefore assumed to be uniformly distributed in the remainder of the body. On the contrary, in the pretargeted mice over 99 %ID was found in the harvested organs or was excreted.

Besides the tumor, in mice injected with CC49-TCO pretargeted ^{177}Lu -**2** the kidney was the only organ to retain ^{177}Lu (1.58 ± 0.14 %ID/g at 3 h). Most of this activity (64%) cleared with a 1.2 h half-life while the rest was eliminated more slowly ($t_{1/2,\beta} = 35.8$ h).



Supplemental Figure 6: Blood clearance of (A) ¹⁷⁷Lu-DOTA-CC49 and (B) CC49-TCO pretargeted ¹⁷⁷Lu-tetrazine 2 in mice bearing colon carcinoma xenografts. Curve fitting according to a two-phase decay (A) or a one-phase decay (B) was performed with GraphPad Prism. The data points are the mean %ID/g ± SD (n = 4).

Supplemental Table 1: Biodistribution of ¹⁷⁷Lu-DOTA-CC49 in mice bearing LS174T colon carcinoma xenografts. Data represent the mean ± SD (n = 4).

organ	3 hours	6 hours	1 day	2 days	3 days	4 days	7 days
	%ID/g						
Tumor	15.79±2.77	23.75±1.69	49.44±6.40	61.68±16.24	73.26±26.69	63.05±9.57	66.57±25.24
(gram tumor)	(0.47±0.09)	(0.43±0.04)	(0.42±0.17)	(0.23±0.10)	(0.49±0.21)	(0.71±0.21)	(0.63±0.49)
Blood	25.86±2.44	24.37±0.63	14.20±1.25	13.23±1.78	6.43±4.11	2.34±1.06	2.92±2.15
Heart	5.53±0.70	5.48±0.91	3.40±0.77	4.39±1.91	1.58±0.90	0.64±0.31	0.79±0.54
Lung	9.90±1.78	8.86±0.76	5.99±0.42	6.53±0.62	3.55±1.94	1.74±0.41	2.10±1.34
Liver	9.13±1.19	9.80±1.19	9.51±3.98	9.92±1.98	13.91±5.92	18.98±3.45	11.56±3.18
Spleen	5.90±1.38	6.29±1.06	4.94±1.26	5.47±0.81	5.15±0.93	5.50±0.90	4.71±1.65
Kidney	6.54±0.43	7.27±0.22	4.21±0.60	4.49±0.51	2.88±1.44	1.67±0.23	1.77±0.38
Bladder	1.15±0.11	2.12±0.66	3.63±0.91	3.80±0.32	2.19±1.12	1.05±0.32	1.01±0.59
Muscle	1.82±0.15	1.21±0.39	1.53±0.63	1.42±0.20	0.76±0.39	0.32±0.14	0.34±0.18
Bone	2.76±0.67	2.21±0.08	1.85±0.46	1.59±0.38	1.40±0.49	0.76±0.15	0.75±0.12
	%ID/organ						
Stomach	0.35±0.06	0.30±0.07	0.25±0.08	0.35±0.10	0.18±0.05	0.07±0.03	0.13±0.09
Sm. intestine	2.54±0.14	2.49±0.18	1.52±0.58	1.95±0.27	0.91±0.38	0.56±0.14	0.64±0.39
Lg. intestine	1.07±0.15	1.24±0.10	0.90±0.23	1.15±0.24	0.85±0.25	0.58±0.12	0.56±0.29

Supplemental Table 2: Biodistribution of CC49-TCO pretargeted ¹⁷⁷Lu-tetrazine in mice bearing LS174T colon carcinoma xenografts. Data represent the mean ± SD (n = 4).

organ	1 hour	3 hours	6 hours	1 day	2 days	4 days	7 days
	%ID/g						
Tumor	4.71±1.13	5.38±0.48	4.53±1.69	3.83±0.95	3.15±1.32	2.06±0.84	1.02±0.36
(gram tumor)	(0.45±0.18)	(0.40±0.07)	(0.40±0.10)	(0.61±0.32)	(0.67±0.31)	(1.04±0.20)	(1.46±0.26)
Blood	0.42±0.20	0.03±0.00	0.02±0.00	0.01±0.00	0.01±0.00	0.00±0.00	0.00±0.00
Heart	0.16±0.05	0.04±0.00	0.03±0.01	0.03±0.00	0.00±0.01	0.02±0.00	0.01±0.00
Lung	0.54±0.15	0.21±0.03	0.11±0.02	0.10±0.01	0.08±0.03	0.06±0.01	0.04±0.01
Liver	0.29±0.08	0.18±0.02	0.15±0.01	0.13±0.02	0.11±0.02	0.14±0.02	0.13±0.03
Spleen	0.17±0.04	0.09±0.01	0.07±0.01	0.07±0.01	0.07±0.01	0.07±0.01	0.08±0.01
Kidney	2.38±0.55	1.58±0.14	1.09±0.18	1.01±0.13	0.49±0.07	0.34±0.02	0.19±0.04
Bladder	2.21±1.15	0.85±0.64	0.20±0.08	0.20±0.06	0.12±0.07	0.13±0.04	0.15±0.02
Muscle	0.23±0.21	0.05±0.03	0.02±0.00	0.02±0.00	0.02±0.01	0.01±0.00	0.01±0.00
Bone	0.43±0.40*	0.17±0.19	0.03±0.00	0.03±0.01	0.02±0.00	0.02±0.01	0.01±0.00
	%ID/organ						
Stomach	0.10±0.10	0.02±0.01	0.01±0.01	0.04±0.05	0.01±0.01	0.01±0.00	0.01±0.00
Sm. intestine	0.38±0.11	0.15±0.04	0.05±0.01	0.06±0.06	0.07±0.08	0.03±0.02	0.02±0.01
Lg. intestine	0.16±0.03	0.22±0.07	0.38±0.26	0.09±0.05	0.06±0.06	0.04±0.04	0.07±0.04

* n = 3

Supplemental Table 3: Residence times (in hours) of ^{177}Lu -DOTA-CC49 and CC49-TCO pretargeted ^{177}Lu -tetrazine in LS174T xenograft bearing mice.

Organ	^{177}Lu-DOTA- CC49	^{177}Lu-Tetrazine
Blood	14.76 ± 5.07	0.067 ± 0.011
Heart wall	0.26 ± 0.13	0.001 ± 0.0005
Lungs	0.82 ± 0.40	0.031 ± 0.004
Liver	28.57 ± 6.74	0.302 ± 0.118
Spleen	0.70 ± 0.11	0.023 ± 0.003
Kidneys	1.40 ± 0.42	0.293 ± 0.044
Uterus	0.53 ± 0.34	0.026 ± 0.017
Ovaries	0.113 ± 0.05	0.0034 ± 0.0015
Muscle	9.96 ± 3.95	0.19 ± 0.11
Bone	5.46 ± 0.95	0.239 ± 0.12
Brain	0.172 ± 0.09	0.001 ± 0.0005
Stomach	0.28 ± 0.13	0.032 ± 0.02
Sm. Intestine	1.50 ± 0.55	0.082 ± 0.04
Lg. Intestine	1.28 ± 0.50	0.23 ± 0.14
Bladder Wall	0.050 ± 0.026	0.009 ± 0.004
Red Marrow	1.18 ± 0.41	0.0054 ± 0.0009
Tumor	50.84 ± 12.30	3.93 ± 1.41

According to Geerlings (4), based on 5.38 %ID/g ^{177}Lu -**2** at 3 h, 6×10^8 cells/g, a maximized ^{177}Lu -DOTA occupation of 25%, and a tumor dose delivery efficiency of 30% (heterogeneous uptake, 6.7 day decay half life), gives 3×10^4 disintegrations per cell, indicating that a therapeutic tumor dose can be delivered with CC49-TCO pretargeted ^{177}Lu -tetrazine **2** in mice.

REFERENCES

1. Rossin R, Renart Verkerk P, van den Bosch S, et al. In vivo chemistry for pretargeted tumor imaging in live mice. *Angew Chem Int Ed Engl.* 2010;49:3375-3378.
2. Theodore LJ, Axworthy DB, Reno JM, Inventors; NeoRx Corporation, Seattle, WA, assignee. Small molecular weight ligand-hexose containing clearing agents. US patent US006075010A.
3. Schwartz AL. The hepatic asialoglycoprotein receptor. *Crit Rev Biochem.* 1984;16:207-233.
4. Geerlings MW. Radionuclides for radioimmunotherapy: criteria for selection. *Int J Biol Markers.* 1993;8:180-186.